Journal of Applied Pharmaceutical Science Vol. 11(02), pp 084-092, February, 2021
Available online at http://www.japsonline.com
DOI: 10.7324/JAPS.2021.110211a
ISSN 2231-3354

# Synthesis, characterization, deoxyribonucleic acid binding and antimicrobial activity of bivalent metal complexes with 2-acetylpyridine isonicotinoylhydrazone

Dhanalakshmi Dornala[1], Hussain Reddy Katreddi[1*], Anuja Kandukuri[1], Srinivasulu Kummara[1], Nagamani Yamaduru Balaramaiah[2]

[1]Department of Chemistry, Sri Krishnadevaraya University, Anantapur, India.
[2]Department of Chemistry, N.S.P.R. Govt. Degree College W, Hindupur, India.

**ARTICLE INFO**

Received on: 11/08/2020
Accepted on: 23/12/2020
Available online: 05/02/2021

***Key words:***
Analysis, bivalent metal complexes, 2-acetylpyridine isonicotinoyhydrazone, DNA interactions, antimicrobial activity.

**ABSTRACT**

Survey of literature revealed that bivalent metal complexes of nitrogenous heterocyles exhibit diverse structural and pharmacological features. The purpose of this study is to investigate structural and biological applications of metal complexes with 2-acetylpyridine isonicotinoylhydrazone (APINH). Hence Co(II), Ni(II), Cu(II) & Zn(II) compounds with APINH were produced and characterized according to Electrospray Ionization Mass Spectrometry (ESI-MS), Fourier Transform Infrared spectroscopy (FT-IR) and electronic spectral data. The copper complex was also studied using electron spin resonance (ESR) spectroscopy. DNA interactions of complexes were investigated by using UV-spectroscopy. The metal derivatives were examined for antimicrobial action across *Bacillus cereus*, *Staphylococcus aureus*, *Escherichia coli & Klebsiella pneumonia* employing agar-well diffusion process. Conductivity data suggest non-electrolytic behaviour of compounds. FT-IR results indicate uni-negative tridonor nature of ligand. UV-Visible data confirms octahedral structure for the complexes. ESR data suggest covalent nature of M─L bond. The data indicate that the nickel derivative sticks to DNA more firmly. Copper compound manifests more effectively than other investigated metal derivatives.

## INTRODUCTION

Metallo-azomethines have received exceptional curiosity of inorganic chemists because of their excellent structural diversity, rigidity, and stability (Angelusiu *et al*., 2010; Aslan *et al*., 2011; Wang *et al*., 2009). Hydrazones have been investigated for the new drug development. Analogous compounds of hydrazones act as anti-tumour agents with the support of suitable carrier proteins (Giraldi *et al*., 1980). The interest in studying metallo-hydrazones has been due to their significant biotic actions.

Isonicotinoylhydrazones (INHs) occupy distinct position in the domain of hydrazones due to their biological and pharmacological applications (Rollas *et al*., 2007). INHs have been used in the treatment of tuberculosis (Cocco *et al*., 1999), cancer (Chitambar *et al*., 1999), and diseases due to the iron overload. INHs were first prepared by Sah and Peoples using isoniazid and suitable carbonyl compound. The composites showed action across the strains of Mycobacterium *tuberculosis*. Due to the synthetic facility, biological potency, and pharmacological activates of isoniazid group several INHs have been synthesized and their transition metal complexes are investigated. The heterocyclic INHs constitute an important class of hydrazones. These hydrazones have attracted the attention of medicinal chemists because of their diverse pharmacological properties covering iron scavenging and anti-tubercular activities (Krishnamoorthy *et al*., 2011). Biological activities of many of these compounds were explained (Patole *et al*., 2003) according to their DNA binding abilities.

Deoxyribonucleic acid (DNA) is the treasury of cellular intelligence that is interfaced uninterruptedly for depositing and distributing essential message for the survival. It has been regarded as an important intracellular prey for chemists who achieve success in developing a new drug for dreadful diseases, particularly for

*Corresponding Author
*Hussain Reddy Katreddi, Department of Chemistry, Sri Krishnadevaraya University, Anantapur, India. E-mail: khussainreddy @ yahoo.co.in*

© 2021 Dhanalakshmi Dornala *et al*. This is an open access article distributed under the terms of the Creative Commons Attribution 4.0 International License (https://creativecommons.org/licenses/by/4.0/).

cancer. Coordination compounds are known to interact with specific sites of DNA. These interactions have been used to access and manipulate functions and cellular information. Metal–DNA interaction is a thrilling area of research because of their potential use in the development of medicines. Significant attempts are being made to investigate Metal–DNA interactions (Moksharagni *et al*., 2017; Suseelamma *et al*., 2018) and to develop drugs. Recently we have reported (Moksharagni *et al*., 2016; Pragathi *et al*., 2013; Srinivasulu *et al*., 2019) structural elucidation of Ln(III)-2-acetylpyridine isonicotinoyl-hydrazine (APINH) complexes and their interaction with DNA. So far transition metal complexes of APINH are not investigated and focused as DNA binding agents and antimicrobial agents. Thus, looking to the significance of metal complexes as DNA binding agents for the successful development of antimicrobial agents, we have studied bivalent metal complexes of APINH and the results are presented in this article.

## MATERIALS AND METHODS

The precursors of APINH were procured from Aldrich company and were utilized as such. LR (Merck) grades metal chlorides & CT DNA bought from Genie Bio labs used in the present study. Remaining are Analytical Reagent chemicals and utilized as such.

### Preparation of ligand (APINH)

Equimolar (5 mmol) quantities of 2-acetylpyridine and isoniazid were taken in a 100-ml RB flask containing 20 ml of methyl alcohol and refluxed for 3 hours. A white colored product was appeared on chilling the flask to room temperature (RT). The product was separated by filtration, cleaned with 5 ml of ethanol, and dried. Yield, 82%, M.P., 163ºC–164ºC. The ligand was recrystallized from ethanol. The preparation of APINH ligand is shown in Figure 1.

### Preparation of complexes

The compounds were produced by combining APINH (1 g, 0.41 mmol) and suitable metal salt (0.41 mmol) in a 100-ml round bottom flask containing 40 ml of methyl alcohol. The reaction mixture was refluxed on water bath up to 3 hours. After 1 hour and on slow evaporation, chromatic complexes were formed, separated by exudation, cleaned with methyl alcohol subsequently by hexane, and dried. Preliminary data of metal derivatives are given in Table 1.

### Equipment

The instruments used in the present study are described by us in our recently published articles (Moksharagni *et al*., 2016).

### DNA binding experiments

Experimental details are given in our recently published article (Nagamani *et al*., 2020).

### Antibacterial activity studies

The bacteria used and protocols employed in this study are given in our recently published article (Srinivasulu *et al*., 2019).

## RESULTS AND DISCUSSION

The ligand (APINH) was easily prepared by reacting 2-acetylpyridine and isoniazid in high yield (82%). APINH is characterized as per analytical data. **Elemental analysis**: C-64.00 (65.02); H-5.00 (5.10); *N*: 23.33 (24.01); IR spectra (KBr) Peaks at 3,189, 1,668, 1,623, 1,581, 991 and 753 $cm^{-1}$ are allocated to $\nu$(NH), $\nu$(C=O) (Amide I), $\nu$(C=N), $\nu$(Py ring), $\nu$(Py bending), and $\gamma$(Py ring oop bending) vibrations, respectively. **$^1$H-NMR spectra:** (in dimethyl sulphoxide (DMSO) solvent); $\delta$ 8.60–8.94 (multiplet

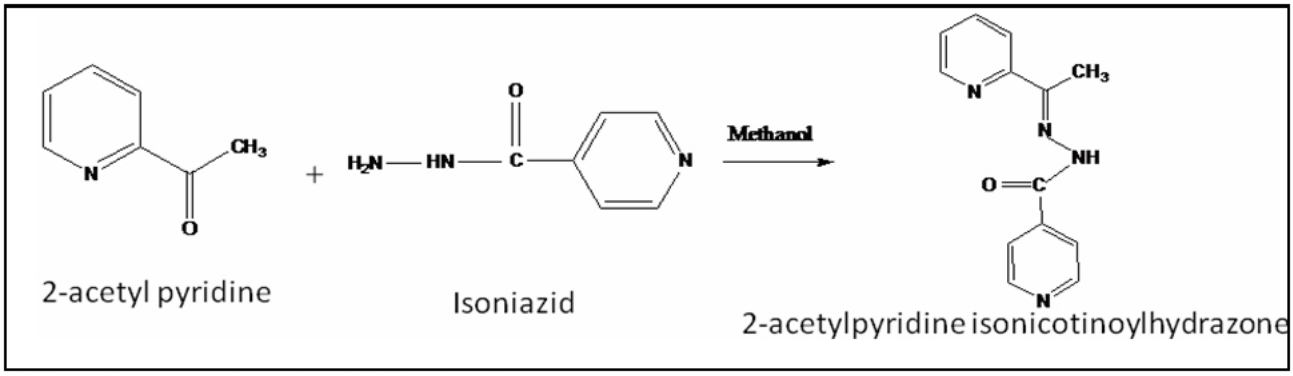


**Figure 1.** Preparation of APINH.

**Table 1.** Primary data of compounds.

| S. No. | Complex and its [Formula] | ESI-MS (F.W)[a] | Melting point (°C) | Color (yield gm) | (Yield %) | Molar conductivity[b] ($\Omega^{-1}cm^2mol^{-1}$) |
|---|---|---|---|---|---|---|
| 1 | $Co(APINH)_2[Co(C_{13}H_{11}N_4O)_2]$ | 537.11 (538.93) | 248–249 | Dark Brown (0.68) | 22.60 | 22.64 |
| 2 | $Ni(APINH)_2[Ni(C_{13}H_{11}N_4O)_2]$ | 537.12 (538.69) | 253–254 | Light Brown (0.52) | 16.10 | 36.51 |
| 3 | $Cu(APINH)_2[Cu(C_{13}H_{11}N_4O)_2]$ | 542.12 (543.54) | 267–268 | Green (0.36) | 35.50 | 20.13 |
| 4 | $Zn(APINH)_2[Zn(C_{13}H_{11}N_4O)_2]$ | 537.12 (543.38) | 235–236 | Yellow (0.58) | 51.60 | |

[a]Theoretical data are given in brackets.

4H), $\delta$ 8.13 (singlet 1H), $\delta$ 7.36–7.62 (multiplet 4H) $\delta$ 3.34 (singlet 3 H), are assigned to pyridine, >NH, isonicotine and $-CH_3$ protons. **Mass spectrum** (Fig. 2) of APINH shows molecular ion peak at (*m/z*) 240. It corresponds to chemical formula $C_{13}H_{12}N_4O$.

The complexes are prepared by reacting APINH with suitable metal chloride. The compounds are not hygroscopic, and solvable in ethyl alcohol and freely in dimethylformamide (DMF) and DMSO. Color, yield, Electrospray Ionization Mass Spectrometry (ESI-MS) and molar conductivity results are delineated in Table 1. Typical ESI-Mass spectrum of $Ni(APINH)_2$ is shown in Figure 3. A peak is observed at 537.12 due to the emergence of $M^+$ peak in conformity with molecular formula, $[Ni(C_{13}H_{11}N_4O)_2]$. Solutions ($1 \times 10^{-3}$M) of complexes were prepared using DMF solvent for measuring the conductivity. Non-electrolytic behavior of complexes is indicated by conductivity results.

**Electronic spectra**

Typical electronic spectrum of $Co(APINH)_2$ complex is depicted in Figure 4. Electronic spectral data and assignment of bands are delineated in Table 2. In the visible spectra of $Co(APINH)_2$, $Ni(APINH)_2$, and $Cu(APINH)_2$ complexes, weak peaks ($\varepsilon$ = 5−10 L. $mol^{-1}$. $cm^{-1}$) are, respectively, observed at 14,044, 13,123, and 14,245 $cm^{-1}$ which are assigned to $^4T_{1g} \rightarrow {}^4T_{2g}$ , $^3A_{2g} \rightarrow {}^3T_{2g}$ and $^2E_g \rightarrow {}^2T_{2g}$ electronic transitions in favor octahedral structure for the complexes (Pragathi *et al*., 2013; Srinivasulu *et al*., 2019).

**Electron spin resonance (ESR) spectral studies**

ESR spectra of Cu(II) complex in solid and solution (in DMF) states were documented at RT and at liquid nitrogen temperature (LNT). Spectra are depicted in Figure 5 and results

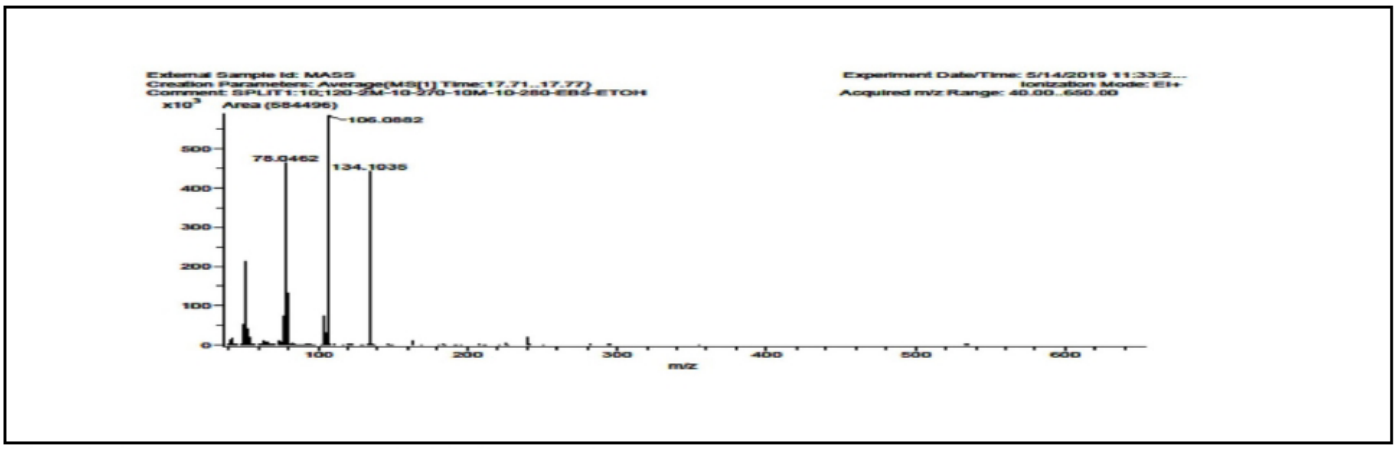


**Figure 2.** Mass spectrum of APINH.

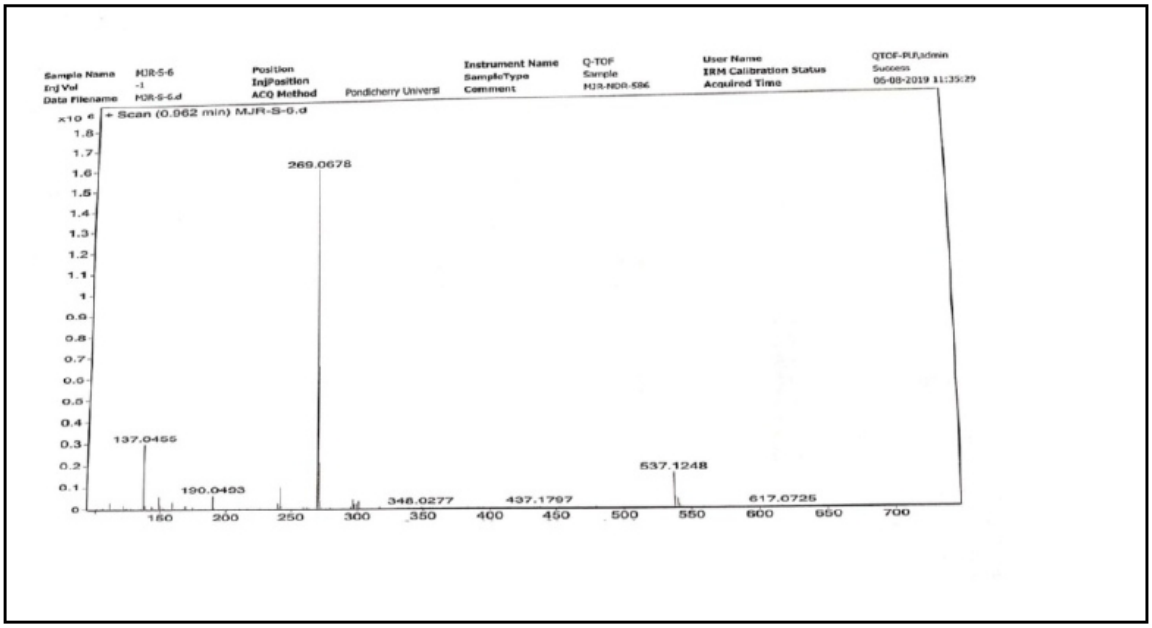


**Figure 3.** ESI-mass spectrum of $Ni(APINH)_2$.

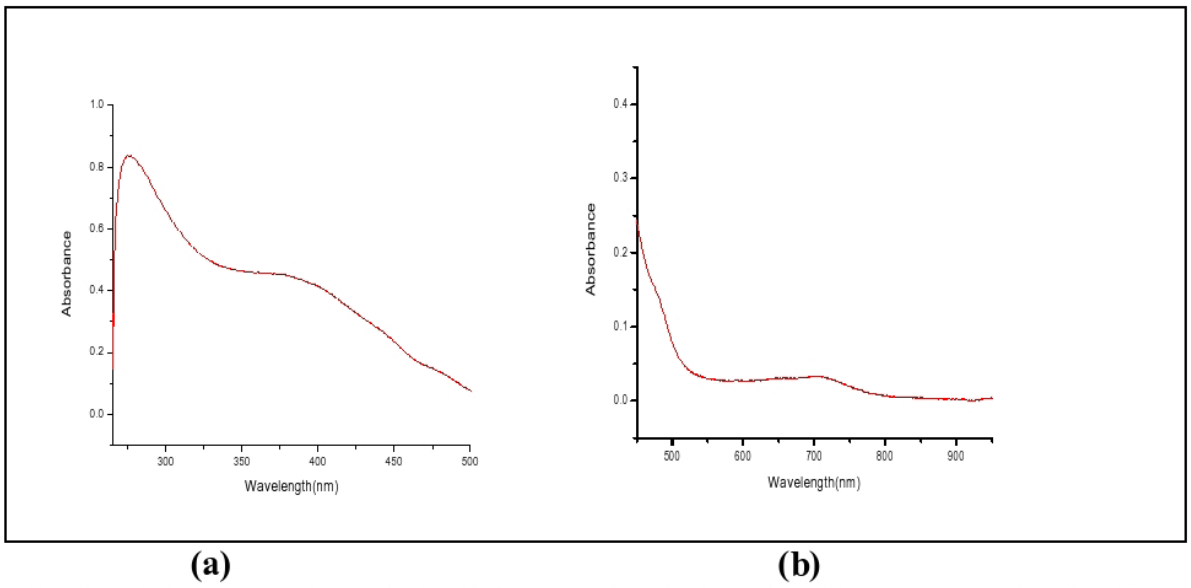


**Figure 4.** Electronic spectra of $Co(APINH)_2$ in (a) in UV at low concentration($1 \times 10^{-4}$M) and (b) in visible region at high concentration ($1 \times 10^{-2}$M).

**Table 2.** Electronic spectral data of compounds.

| S. No | Complex | Wavelength λ max (nm) | Frequency ($cm^{-1}$) | Assignment |
|---|---|---|---|---|
| | | 275 | 36,363 | $\pi$–$\pi$* Transition |
| 1 | $Co(APINH)_2$ | 377 | 26,525 | Charge transfer transition |
| | | 712 | 14,044 | d–d transition |
| | | 279 | 35,842 | $\pi$–$\pi$* Transition |
| 2 | $Ni(APINH)_2$ | 307 | 32,573 | Charge Transfer Transition |
| | | 762 | 13,123 | d-d transition |
| | | 272 | 36,764 | $\pi$–$\pi$* Transition |
| 3 | $Cu(APINH)_2$ | 381 | 26,246 | Charge transfer transition |
| | | 702 | 14,245 | d–d transition |

**Table 3.** ESR spectral data of $Cu(APINH)_2$.

| | ESR spectral parameters[a] | | | | | | | | | |
|---|---|---|---|---|---|---|---|---|---|---|
| State | $g_{\parallel}$ | $g_{\perp}$ | $g_{ave}$ | $G$ | $A_{\parallel}\times10^{-5}$ | $A_{\perp}$ x 10-5 | $K_{\parallel}$ | $K_{\perp}$ | $\lambda$ | $\alpha^2$ |
| Solid | 2.15 (2.15) | 2.05 (2.05) | 2.08 (2.08) | 3.09 (3.09) | – | – | 0.985 | 0.866 | 513 | – |
| Solution | 2.29 (2.10) | 2.03 (2.03) | 2.11 (2.05) | 10.38 (3.53) | 0.00146 | 0.00068 | 0.9896 | 1.09 | 951 | 0.697 |

[a]ESR spectral data of $Cu(APINH)_2$ in Solid and solution state at LNT (RT data are given in parenthesis).

are delineated in Table 3. Using tetracyanoethylene (TCNE) radical as reference the 'g' values of complex were calculated.

*Solid state ESR spectra*

The *g* parallel and *g* perpendicular data of $Cu(APINH)_2$ compound are located at 2.15 and 2.05, respectively. The $g_{\parallel}$ value (less than 2.3) of complex suggests covalent character in M-L bond (Hussain Reddy *et al*., 1999). The trend, $g_{\parallel} > g_{\perp} > 2.0023$ suggest that the single electron mostly resides in $d_x2_{-y}2$ orbital which is considered as a trait of octahedral structure for the complex. The axial symmetry parameter *G* may be evaluated by applying the formula

$$G = \frac{(g_{\parallel} - 2.003)}{(g_{\perp} - 2.003)}$$

The calculated *G* value for the complex is found to be 3.0 which indicates non-appearance of misalignment of molecular axes and exchange coupling.

*Solution state*

Spectra of $Cu(APINH)_2$ compound are depicted in Figure 5. Spectrum recorded at LNT exhibits well separated peaks in low field & in high field regions matching to $g_{\parallel}$ and $g_{\perp}$ sequence.

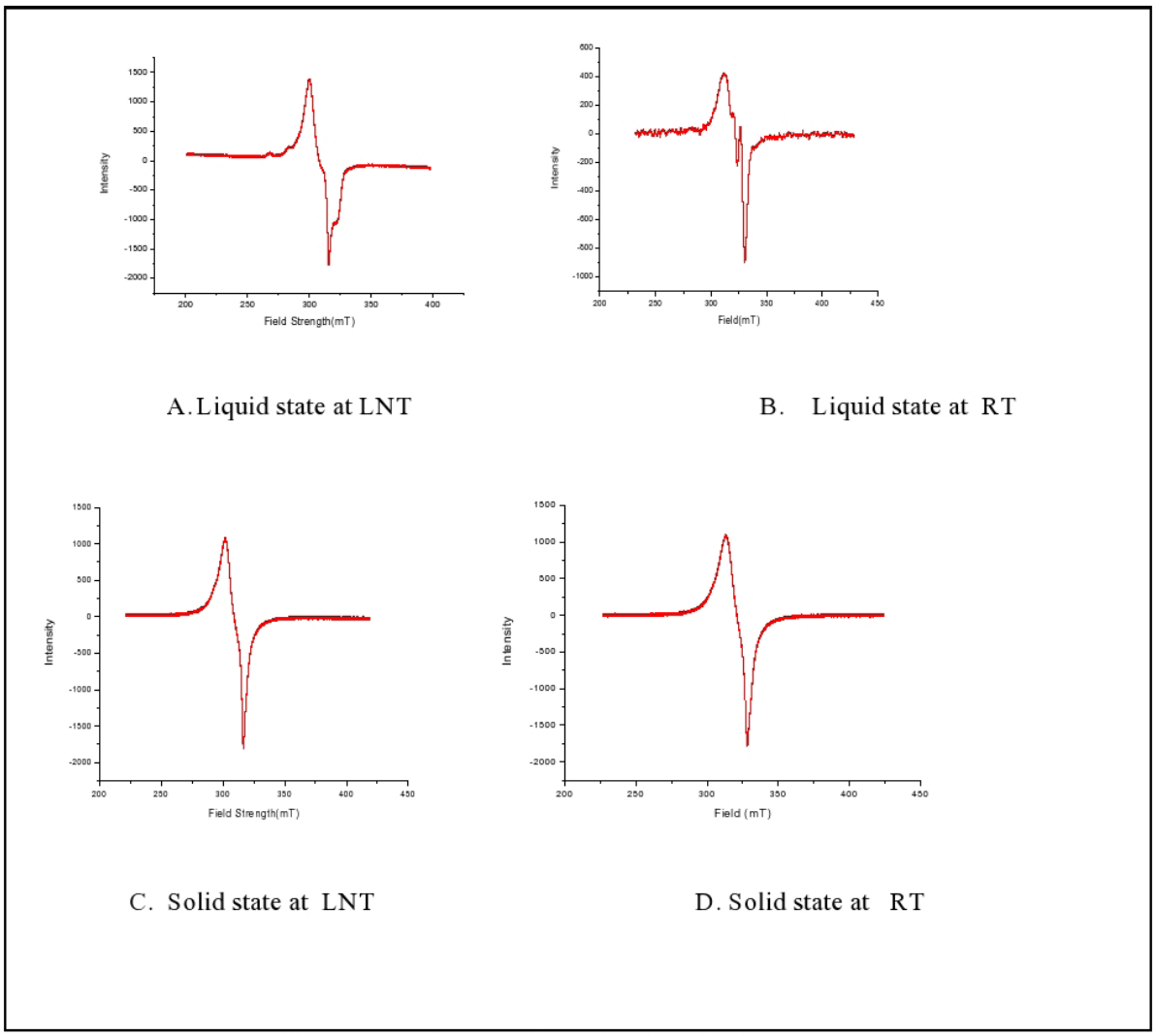


**Figure 5**. ESR spectra of $Cu(APINH)_2$ (A) In solution state at LNT; (B) In solution state at RT; (C) In solid state at LNT and (D) In solid state at RT.

Important spectral data, $g_{\|}$, $g_{\perp}$, $g_{ave}$, $G$, $A_{\|}$ (separation between two adjacent $g_{\|}$ peaks), $A_{\perp}$ (separation between two adjacent $g_{\perp}$ peaks), $K_{\|}$ and $K_{\perp}$ (orbital reduction parameters), λ (spin-orbit constant) and $\alpha^2$ (covalent factor) are calculated and data are summarized in Table 3. The $K_{\|}$ & $K_{\perp}$ are determined utilizing equations given below

$$g_{\|} = \frac{g_e - 8\,K_{\|}^2\lambda}{\Delta E(d\text{-}d)}$$

$$g_{\perp} = \frac{g_e - 2K_{\perp}^2\lambda}{\Delta E(d\text{-}d)}$$

According to Hathaway, $K_{\|} = K_{\perp} = 0.77$, $K_{\|} < K_{\perp}$, and $K_{\|} > K_{\perp}$ for pure $\sigma$ binding, for in-plane π-binding and for out-plane π-binding, respectively. For the present copper compound $K_{\|}$ and $K_{\perp}$ are 0.989 and 1.09 sequentially. For this copper compound, the $K_{\|}$ value is less than $K_{\perp}$. This trend indicates the appearance of in-plane π-binding. Covalent factor ($\alpha^2$), is calculated using equation given below.

$$\alpha^2 = A_{\|}/p + (g_{\|} - 2.0023)3/7(g_{\perp} - 2.0023) + 0.004$$

Data (Table 3) advise covalent nature (Wertz *et al.*, 1986) of metal ligand bond.

**Infrared spectra**

IR spectrum of APINH is juxtaposed with its metal compounds to reveal donating atoms. Selected IR peaks and their allocations are presented in Table 4. The IR spectrum of the APINH shows main peaks at 3,189 and 1,668 $cm^{-1}$ due to $\nu_{N\text{-}H,}$ and $\nu_{C=O}$ stretching modes. Such peaks are absent in spectra of metal compounds due to enolization followed by complex formation with metal ions. In the spectra of compounds, a new peak present in the 1,022–1,170 $cm^{-1}$ range is assigned to $\nu_{C\text{-}O}$ vibration. A strong (and new) peak is noticed in the spectra of all the compounds in 1,592–1,635 $cm^{-1}$ range due to azomethine ($\nu_{C=N}$) involved in coordination. Results revealed that the APINH functions as uni-negative tridonor ligand in all the compounds. New peaks in 596–554 and 498–461 $cm^{-1}$ range are allocated to $\nu_{(M\text{-}O),}$ and $\nu_{(M\text{-}N)}$ stretching vacillations sequentially.

**Table 4**. Selected IR data ($cm^{-1}$) of APINH and its metal compounds.

| APINH | $Co(APINH)_2$ | $Ni(APINH)_2$ | $Cu(APINH)_2$ | $Zn(APINH)_2$ | Assignment |
|---|---|---|---|---|---|
| 3,189 | – | – | – | – | $\nu_{NH}$ |
| 1,668 | – | – | – | – | $\nu_{C=O}$ |
| – | 1,604 | 1,592 | 1,618 | 1,635 | $\nu_{C=N}$ |
| | 1,170 | 1,062 | 1,022 | 1,162 | $\nu_{C-O}$ |
| | | | | 1,067 | |
| | 596 | 569 | 567 | 554 | $\nu_{M-O}$ |
| | 491 | 488 | 461 | 498 | $\nu_{M-N}$ |

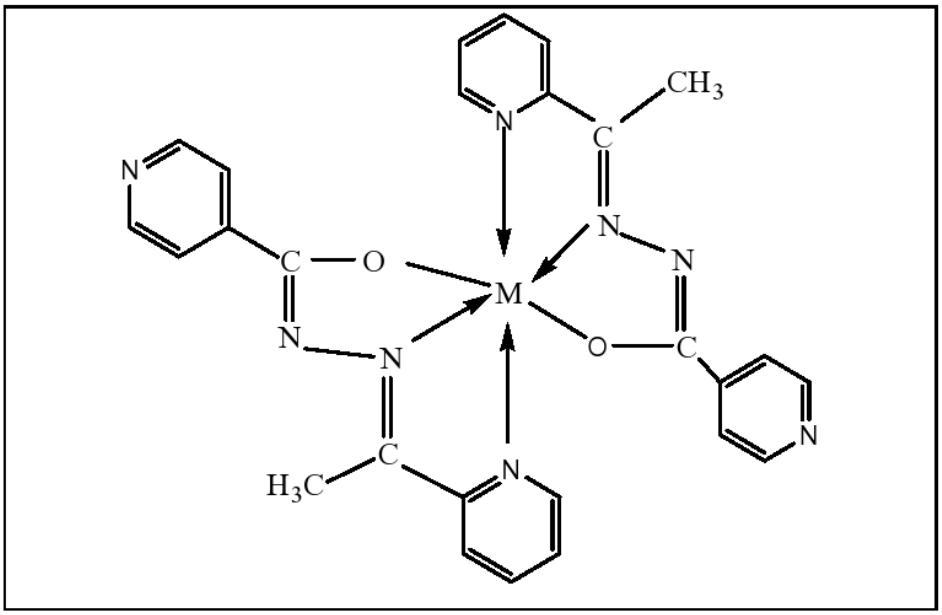


**Figure 6**. A common proposed structure for complexes [M = Co(II), Ni(II),Cu(II) and Zn(II)].

**Table 5.** CV data of bivalent metal complexes.

| S. No | Complex | Redox couple | $E_{pc}$ | $E_{pa}$ | $\Delta Ep$ (mV) | $E_{1/2}$ | $-i_c/i_a$ | LogKc[a] | $-\Delta G^b$ |
|---|---|---|---|---|---|---|---|---|---|
| 1 | $Co(APINH)_2$ | II/I | −1.03 | −0.566 | 464 | −0.798 | 1.863 | 0.071 | 412 |
| 2 | $Ni(APINH)_2$ | II/I | −1.07 | −0.60 | 470 | −0.835 | 2.120 | 0.072 | 416 |
| 3 | $Cu(APINH)_2$ | II/I | −0.032 | 0.523 | 555 | +0.277 | 1.652 | 0.060 | 347 |
| 4 | $Zn(APINH)_2$ | II/I | −1.132 | −0.464 | 668 | −0.798 | 1.872 | 0.050 | 288 |

[a]$\log K_c = 0.434ZF/RT\Delta E_p$
[b]$\Delta G^o = -2.303RT\log K_c$

In accordance with preliminary and chromatic data, a common structure (Fig. 6) for the compounds is suggested.

## Cyclic voltammetry (CV)

Electrochemistry of metal-compounds was explored by utilizing CV in DMF using 0.1 M $(CH_3CH_2CH_2CH_2)_4N(PF_6)$ as electrolyte. Voltammogram of $Ni(APINH)_2$ compound is depicted in Figure 7 and related CV results are given in Table 5.

The observed cathodic peaks currents do not depend on scan rate. Replicated recordings at 5, 10, and 20 mV. $S^{-1}$ suggests that the metal complexes are stable even in solution state. The $E_{1/2}$ values of metal complexes are found to be in +0.277 to −0.835 V range. Dissimilar currents of +ve and −ve peaks indicate nearly-reversible behavior. The variation, ΔEp in all the complexes be more than 59/*n* mV (where, *n* = aggregate of electrons participated in redox reaction), suggesting nearly-reversible nature of electron transfer (Pragathi *et al*., 2014).

## DNA interaction studies

The interactivity of coordination compounds with calf-thymus DNA was tracked by absorption (UV-Visible) spectroscopy. Spectra (Fig. 8) were recorded in 250–500 nm range with and without DNA. The concentrations of CT-DNA and metal complexes utilized, respectively, are $53 \times 10^{-6}$ M and $20 \times 10^{-6}$M. Metal complexes showed strong peak in UV region due to M→L CT transition. The difference in absorbance with raising quantities of CT-DNA was

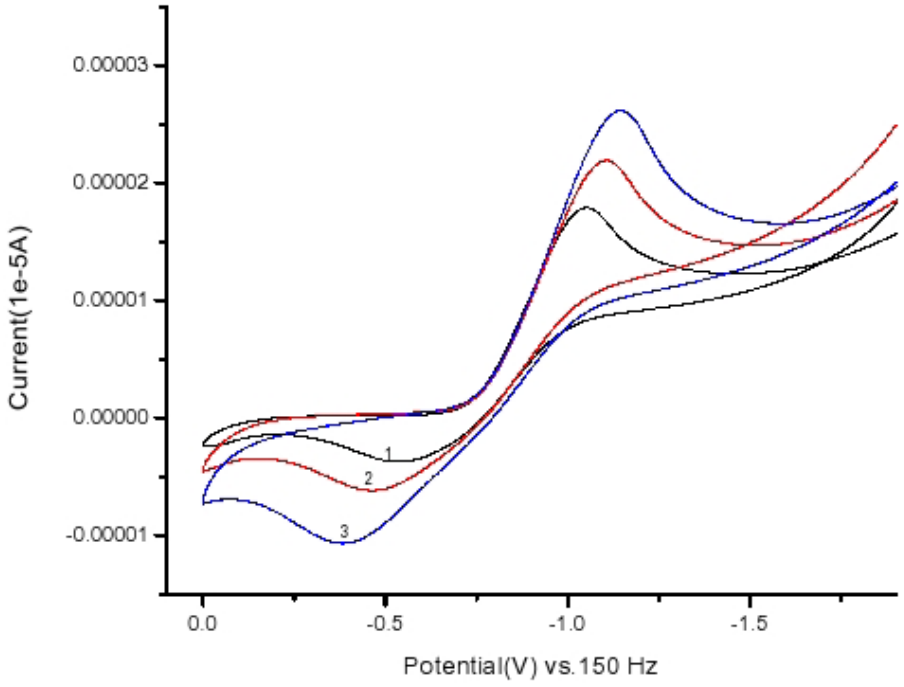


**Figure 7**. Cyclic voltammogram of $Ni(APINH)_2$ scan rates: curve 1, 5; curve 2, 10; curve 3, 20 $mV.S^{-1}$).

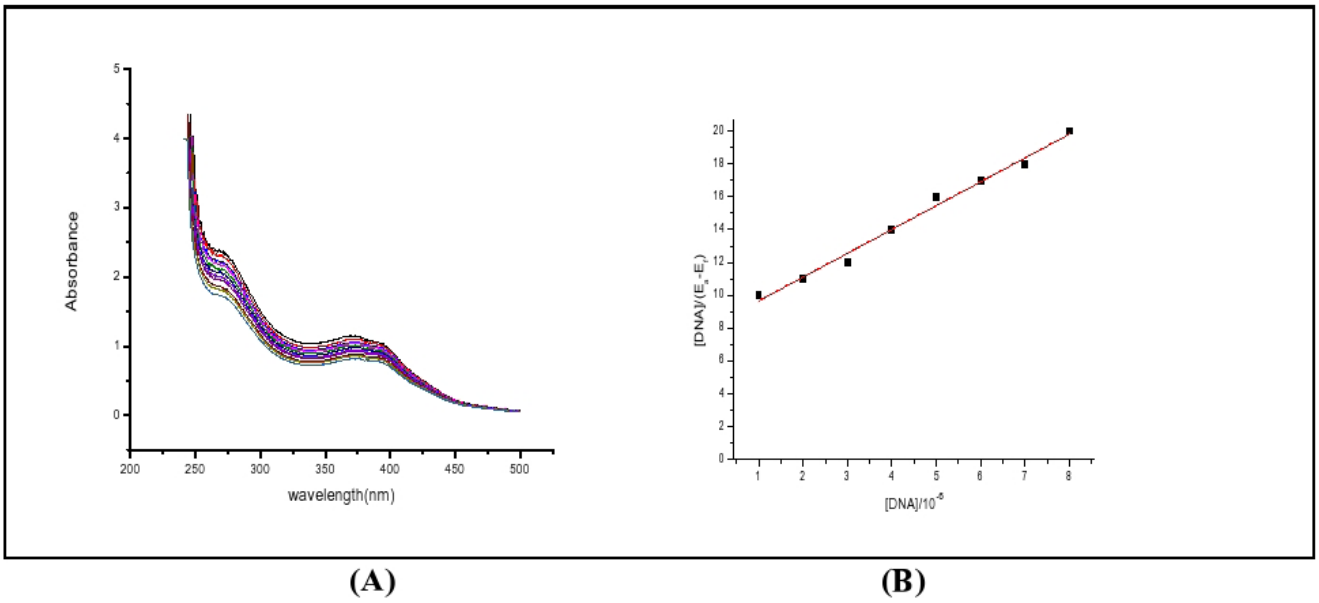


**Figure 8**. (A) Absorption spectra of $Co(APINH)_2$ in the absence(top curve) and in the presence of raising amounts of DNA (B) A plot $[DNA]/(\varepsilon_a-\varepsilon_f)$ versus $[DNA] \times 10^{-6}$.

utilized to judge inherent binding constant ($K_b$), for complexes. The $K_b$ data of the metal compounds are estimated by using modified equation (Wolfe *et al*., 1987) and results are delineated in Table 6.

With raising amounts of CT-DNA, the spectra of metal compounds show bathochromic shift ($\Delta \lambda_{max}$ = 0.5–1.0 nm). The determined $K_b$ values are found in the range 2.5–3.5 × $10^5$ $M^{-1}$.

Metal derivatives that cohere to DNA by intercalation generally show hypochromism and bathochromism or hypsochromism. Electrostatic attraction, hydrogen bonding and groove (minor or major) binding causes hyperchromism. Small bathochromic shifts and low $K_b$ values of present complexes are suggestive of groove binding with DNA in analogy with previous observation (Ramakrishnan *et al*., 2011). The binding constant order is delineated below:

$Cu(APINH)_2$ < $Zn(APINH)_2$ < $Co(APINH)_2$ < $Ni(APINH)_2$

The sequence indicates that the $Ni(APINH)_2$ complex tie up with DNA more firmly.

**Table 6.** Spectral data upon addition of CT-DNA to the compounds.

| S. No | Complex | λmax (nm) | | Δλ | *H*% | $K_b$ [$M^{-1}$] |
|---|---|---|---|---|---|---|
| | | Free | Bound | | | |
| 1 | $Co(APINH)_2$ | 375 | 375.5 | 0.5 | 21.27 | $2.8 \times 10^5$ |
| 2 | $Ni(APINH)_2$ | 356 | 357 | 1.0 | 28.19 | $3.5 \times 10^5$ |
| 3 | $Cu(APINH)_2$ | 357 | 357.5 | 1.0 | 18.53 | $2.5 \times 10^5$ |
| 4 | $Zn(APINH)_2$ | 346 | 346.5 | 0.5 | 17.57 | $2.7 \times 10^5$ |

**Table 7.** Antimicrobial activity data of metal complexes.

| S. No | Sample | Treatment (concentration) | *E. coli* (Mean ± SE) | *K. pneumonia* (Mean ± SE) | *S. aureus* (Mean ± SE) | *B. cereus* (Mean ± SE) |
|---|---|---|---|---|---|---|
| 1 | S-Ciprofloxacin | (5 µg/µl) | 10.50 ± 0.02 | 09.80 ± 0.09 | 10.03 ± 0.03 | 12.16 ± 0.05 |
| 2 | $Co(APINH)_2$ | 100 µg/µl | 1.18 ± 0.02 | 1.17 ± 0.03 | 1.78 ± 0.01 | 1.14 ± 0.01 |
| | | 200 µg/µl | 1.37 ± 0.01 | 1.47 ± 0.02 | 1.80 ± 0.05 | 1.45 ± 0.02 |
| | | 300 µg/µl | 1.62 ± 0.02 | 1.93 ± 0.04 | 1.97 ± 0.02 | 1.87 ± 0.03 |
| 3 | $Ni(APINH)_2$ | 100 µg/µl | 2.25 ± 0.04 | 2.27 ± 0.02 | 2.04 ± 0.02 | 2.01 ± 0.02 |
| | | 200 µg/µl | 2.34 ± 0.04 | 2.30 ± 0.01 | 2.15 ± 0.03 | 2.13 ± 0.02 |
| | | 300 µg/µl | 2.68 ± 0.02 | 2.47 ± 0.01 | 2.36 ± 0.04 | 2.20 ± 0.02 |
| 4 | $Cu(APINH)_2$ | 100 µg/µl | 5.10 ± 0.02 | 4.20 ± 0.05 | 4.10 ± 0.06 | 5.15 ± 0.02 |
| | | 200 µg/µl | 5.47 ± 0.02 | 4.37 ± 0.05 | 4.34 ± 0.06 | 5.25 ± 0.02 |
| | | 300 µg/µl | 5.78 ± 0.01 | 4.53 ± 0.05 | 4.50 ± 0.06 | 5.40 ± 0.02 |
| 5 | $Zn(APINH)_2$ | 100 µg/µl | 2.01 ± 0.01 | 2.07 ± 0.07 | 2.30 ± 0.01 | 2.30 ± 0.05 |
| | | 200 µg/µl | 2.40 ± 0.02 | 2.13 ± 0.01 | 2.41 ± 0.01 | 2.71 ± 0.01 |
| | | 300 µg/µl | 2.55 ± 0.03 | 2.25 ± 0.02 | 2.73 ± 0.02 | 2.83 ± 0.01 |

Values are the mean ± SE of inhibition zone in mm.

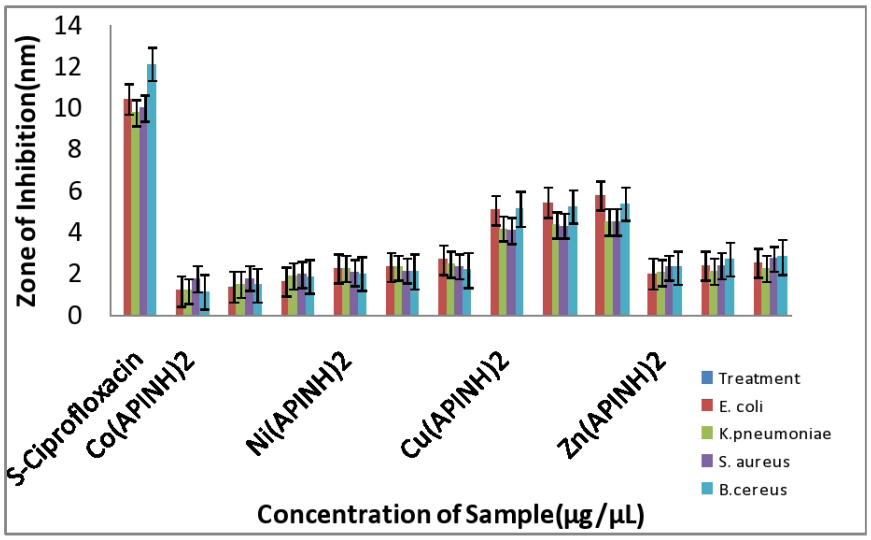


**Figure 9.** Graphical representation of antibacterial activity of metal complexes against pathogenic bacterial strains.

*Antibacterial activity studies*

The compounds were checked for antimicrobial activity across bacterial strains viz. *Escherichia coli, Klebsiella pneumonia*, *Staphylococcus aureus*, and *Bacillus cereus*. Inhibition zones were estimated with 100, 200, and 300 µg/well of complexes by using ciprofloxacin as a reference. The width of inhibition zones (in mm) is evaluated as described before (Srinivasulu *et al*., 2019). Table 7 delineates results.

Activities of coordination compounds are compared using bar graph (Fig. 9). The activity of $Cu(APINH)_2$ complex is more significant.

## CONCLUSION

Spectral results indicate that APINH acts as mono anionic tridonor species and the coordination compounds are assigned to have octahedral structure. Voltammetric investigations suggest that all the compounds undergo quasi-reversible $1e^-$ reduction. Dissimilar currents of cathodic and anodic peaks indicate quasi-reversible conduct of compounds. DNA binding constants ($K_b$) and variation in spectra of metal-compounds suggest groove binding. Copper complex shows the higher antibacterial activity.

## ACKNOWLEDGEMENTS

KHR is grateful to UGC for the award of UGC-BSR Faculty Fellowship. The authors would like to thank KITS, Coimbatore for sending ESI-Mass spectral data of complexes.

## CONFLICT OF INTEREST

The authors declare no conflict of interest.

## FUNDING

University Grants Commission(UGC), New Delhi.

## REFERENCES

Angelusiu V, Barbuceanu SF, Draghici C, Almajan GL. New Cu(II), Co(II), Ni(II) complexes with aroyl-hydrazone based ligand. Synthesis, spectroscopic characterization and *in vitro* antibacterial activity. Eur J Med Chem, 2010; 45:2055–62.

Aslan HG, Ozcan S, Karacan N. Synthesis, characterization and antimicrobial activity of salicylaldehyde benzenesulfonylhydrazone (Hsalbsmh)and its Nickel(II), Palladium(II), Platinum(II), Copper(II), Cobalt(II) complexes. Inorg Chem Commun, 2011; 14:1550–3.

Chitambar CR, Boom P, Wereley JP. Evaluation of transferrin and gallium-pyridoxal isoicotinoyl hydrazone as potential therapeutic agents to overcome lymphoid leukemic cell resistance to gallium nitrate. Clin Cancer Res, 1999; 2:1009–15.

Cocco MT, Congiu C, Onnis V, Pusceddu MC. Synthesis and antimycobacterial activity of some isonicotinoylhydrazones. Eur J Med Chem. 1999; 34:1071–6.

Giraldi T, Goddard PM, Nisi C, Sigon F. Antitumor activity of hydrazones and adducts between aromatic aldehydes and p - (3,3-Dimethyl-1 -triazeno) benzoic acid hydrazide J Pharm Sci, 1980; 69:97–8.

Hussain Reddy K, Sambasiva Reddy P, Babu PR. Synthesis, spectral studies and nuclease activity of mixed ligand copper(II) complexes of heteroaromatic semicarbazones/thiosemicarbazones and pyridine. J Inorg Biochem, 1999; 77:169–76.

Krishnamoorthy P, Sathyadevi P, Senthilkumar K, Muthiah PT, Ramesh R, Dharmaraj N. Copper(I) hydrazone complexes: synthesis, structure, DNA binding, radical scavenging and computational studies. Inorg Chem Commun, 2011; 14:1318–22.

Moksharagni B, Hussain Reddy K. Spectral characterization and DNA binding properties of lanthanide(III) complexes with 2-acetylpyridine isonicotinoylhydrazone. Bull Chem Soc Ethiop, 2016; 30:221–30

Moksharagni B, Rishitha M, Hussain Reddy K. Synthesis, DNA binding properties and antibacterial activity of lanthanide complexes with 2-benzoylpyridine isonicotinoylhydrazone. Indian J Chem, 2017; 56A:232–7.

Nagamani YB, Hussain Reddy K, Anuja K, Srinivasulu K, Dhanalakshmi D. Antibacterial activity and DNA binding properties of bivalent metal complexes with *p*- dimethylaminio- benzaldehyde acetoylhydrazone. Res J Chem Environ, 2020; 24:1–9.

Patole J, Sandbhor PU, Padhye S, Deobagkar DN, Anson CE, Powell A. Structural chemistry and *in vitro* antitubercular activity of acetylpyridine benzoylhydrazone and its copper complex against mycobacterium smegmatis. Bioorg Med Chem Lett, 2003; 13:51–5.

Pragathi M, Husssain Reddy K. Synthesis, crystal structures, DNA binding and cleavage activity of water soluble mono and dinuclear copper(II) complexes with tridentate ligands. Inorganica Chim Acta, 2014; 413:174–86.

Pragathi M, Hussain Reddy K. Synthesis, spectral characterization and DNA interaction of copper(II) and nickel(II) complexes with unsymmetrical Schiff base ligands. Indian J Chem**,** 2013; 52A:845–53.

Ramakrishnan S, Suresh E, Riyasdeen A, Akbarsha MA, Palaniandvar M. Interaction of *rac*-[M(diimine)3] 2+ (M = Co, Ni) complexes with CT DNA: role of 5,6-dmp ligand on DNA binding and cleavage and cytotoxicity. Dalton Trans, 2011; 40:3245–56.

Rollas S, Kuçukguze GS. Biological activities of hydrazone derivatives. Molecules, 2007; 12:1910–39.

Srinivasulu K, Hussain Reddy K, Anuja K, Dhanalakshmi D. DNA binding properties and antibacterial activity of heterolyptic transition metal complexes with 2, 2-bipyridyl and 2-acetylthiophene thiosemicarbazone. Asian J Chem, 2019; 31: 1905–12.

Suseelamma A, Raja K, Hussain Reddy K. Synthesis, characterization, DNA binding and nuclease activity of cobalt(II) complexes of isonicotinoyl hydrazones. Iran J Chem Chem Eng, 2018; 37:63–74.

Wang Q, Yang ZY, Qi GF. Crystal structures, DNA-binding studies and ntioxidant activities of the Ln(III) complexes with 7-methoxychromone3- carbaldehyde-isonicotinoyl hydrazone. Biometals, 2009; 22:927–40.

Wertz JE, Bolton JR. Electron spin resonance- elementary theory and practical applications. 2nd edition, Wiley, New York, NY, p 277, 1986.

Wolfe A, Shimer GH, Meehan T. Polycyclic aromatic hydrocarbons physically intercalate into duplex regions of denatured DNA. Biochemistry, 1987; 26:6392–6.

**How to cite this article:**
Dornala D, Katreddi HR, Kandukuri A, Kummara S, Balaramaiah NY. Synthesis, characterization, deoxyribo-nucleic acid binding and antimicrobial activity of bivalent metal complexes with 2-acetylpyridine isonicotinoyl hydrazine. J Appl Pharm Sci, 2021;11 (02):084-092